Contract No:

This document was prepared in conjunction with work accomplished under Contract No. DE-AC09-08SR22470 with the U.S. Department of Energy (DOE) Office of Environmental Management (EM).

Disclaimer:

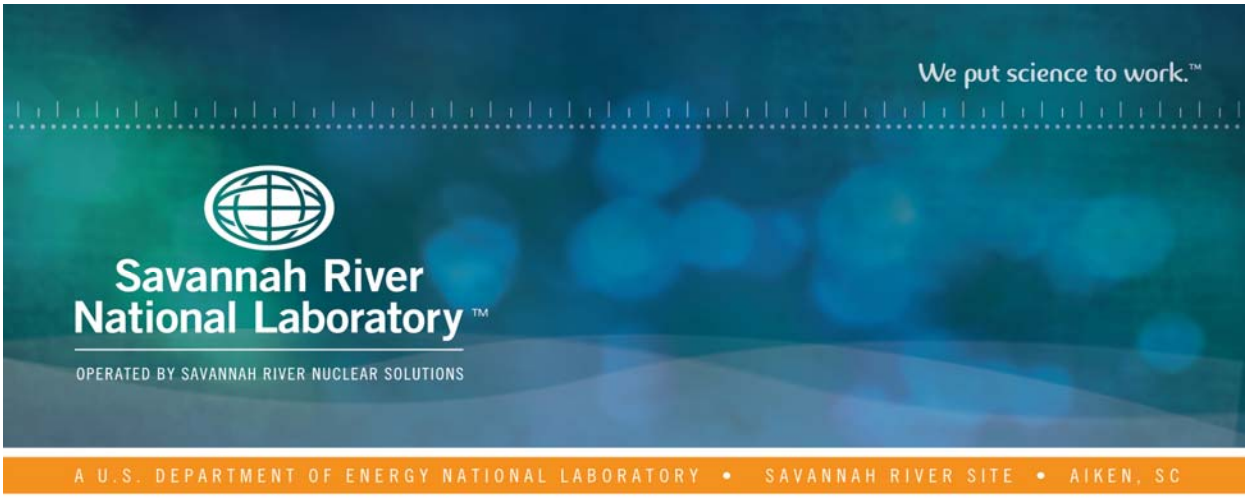

Summary of Recent Raman Spectroscopy Testing of SRS Processes

F. F. Fondeur

R. J. Lascola

P. E. O'Rourke

January 2016

SRNL-STI-2015-00643, Revision 0

DISCLAIMER

Printed in the United States of America

Prepared for
U.S. Department of Energy

SRNL-STI-2015-00643
Revision 0

Keywords: *TCE, Hydrogen, Aluminum, NO_x, Online, Tank Farm, H-Canyon*

Retention: *Permanent*

Summary of Recent Raman Spectroscopy Testing of SRS Processes

F. F. Fondeur

R. J. Lascola

P. E. O'Rourke

January 2016

Prepared for the U.S. Department of Energy under contract number DE-AC09-08SR22470.

Savannah River National Laboratory™

OPERATED BY SAVANNAH RIVER NUCLEAR SOLUTIONS

REVIEWS AND APPROVALS

AUTHORS:

F. F. Fondeur, Advanced Characterization and Processing Date

R. J. Lascola, Analyical R&D Prog & Mat Char Date

P. E. O'Rourke, Analyical R&D Prog & Mat Char Date

TECHNICAL REVIEW:

D. T. Hobbs, Environmental Stewardship Date

APPROVAL:

S. D. Fink, Senior Advisory Engineer, Hanford Missions Programs Date

C. C. Herman, Manager Date
Hanford Missions Programs

EXECUTIVE SUMMARY

This report describes several scoping projects conducted at SRNL using Raman spectroscopic methods for monitoring different aspects of nuclear waste and materials processing. One project examined the suitability of a Raman telescope for in situ measurement of solid residues in waste tanks. Characteristics evaluated for this equipment included radiation resistance, ease of use, and sensitivity. A second project monitored the nitrate content in liquid filtrate from the testing of a rotary microfilter using a fiber-based insertion probe. The third project made Raman measurements of various gases, including H_2 and NO_x, in the headspace of a vessel while dissolving aluminum coupons in nitric acid. Measurements followed the evolution of these species in real time. Although the majority of these projects occurred in the laboratory environment, SRNL has substantial experience with implementing other optical techniques into nuclear materials processing environments. The work described in this report shows the potential of the Raman technology to provide real time measurements of species such as nitrate or hydroxide during sludge washing or evolved gases such as hydrogen or NOx during waste processing.

TABLE OF CONTENTS

LIST OF TABLES

LIST OF FIGURES

LIST OF ABBREVIATIONS

FTIR	Fourier Transform Infra-Red Spectroscopy
FT-Raman	Fourier Transform Raman Spectroscopy
RSD	Relative Standard Deviation or the absolute value of the Coefficient of Variation
SHT	Solvent Hold Tank
SRNL	Savannah River National Laboratory
SVOA	Semi-Volatile Organic Analysis
SRS	Savannah River Site
TCE	Trichloroethene
WTP	Waste Treatment and Immobilization Plant

1.0 Introduction

The Savannah River Site (SRS) stores, processes, and immobilizes high-level radioactive waste produced from reprocessing of irradiated nuclear materials. The waste exists in solid and liquid forms with a number of unit operations used to safely manage and convert the waste into stabilized forms for disposition. Separation processes used at SRS include evaporation, filtration, chemical species extraction (via ion exchange and solvent extraction), aluminum leaching, and precipitation. The efficiencies of these processes are determined almost exclusively by chemical analysis of offline samples. The current sampling methods for sludge and supernate are expensive, may be inadequate if the system features heterogeneous chemical phases, subjects personnel to radiation exposure, and requires substantial precautions for safe operation.

The risks associated with offline sampling and analysis can be reduced by developing and implementing in-line, real-time spectroscopic monitoring methods. The advantages associated with these methods include:

- shorter processing time due to a reduction in the number of analytical hold points,
- opportunity to detect batch variability and heterogeneity,
- more efficient processing with faster detection of end points (and associated reduction in chemical addition) in washing, rinsing, or flushing operations, “real time” detection of any chemical changes, and
- reduce worker exposure to radiation and hazardous chemicals.

Raman spectroscopy is an attractive analytical method for use in remote and hazardous environments. The Raman technique provides material identification and quantitation for a wide variety of chemical species in solution, solid and gas phases based on vibrational spectroscopy. For example, the method can readily measure oxyanions such as nitrate, nitrite, hydroxide, phosphate, sulfate, carbonate, chromate, and oxalate[1] that are important chemical species in nuclear waste supernates, saltcakes, and sludges. The method is relatively easy to implement in remote environments through the use of fiber optics. Raman spectroscopy can also be used to directly detect flammable gases such as hydrogen and hydrocarbons as well as other gases (e.g., oxygen, carbon monoxide, carbon dioxide, and NO_x).

Table 1 provides a list of possible application areas for the deployment of Raman–based analytical systems. These applications cover the analysis of solids, liquids, and gases.

Table 1 Suggested areas for Raman technology deployment

Application Area	Raman Probe Type
Aluminum Leaching Process[2]	Liquid
Corrosion Monitoring of Supernate	Liquid
Glass Melting (DWPF) [3]	Telescope
Tank Closure (Residual Heel Characterization)	Telescope
Spent Fuel Digestion Vapors	Gas cell
Evaporator Overheads	Gas cell
TCE – Contaminated Soils	Gas cell

As part of an ongoing effort to develop technology applicable to monitoring SRS waste processing activities, SRNL has conducted a number of studies exploring the suitability of Raman spectroscopy for in-line and remote measurements. In-line analysis of solutions with fiber-based probes eliminates concerns associated with sampling and has the potential to generate results quickly enough to serve as

input for active process control. A similar use exists for real-time analysis of gases in tank headspace, with the additional potential to raise alarms or trigger responses if incipient flammable conditions occur. Stand-off interrogation of solids and liquids is possible using a Raman probe coupled to a telescope. Such a system could prove useful for chemical identification of solids and liquids inside waste tanks, where sampling and off-line analysis is difficult and hazardous. In cases where the system features liquid mixing, an in-line liquid Raman probe has a lower risk of measuring "outliers" from incompletely, or poorly, mixed systems. In addition, the "real time" feature of an in-line system proves valuable in detecting chemical process deviations. The following sections present descriptions of the features of the Raman-based systems and key findings from each of these projects.

2.0 Discussion

2.1 Raman Telescope Testing

An ongoing activity at SRS is closing high-level waste tanks. This process requires analysis of the residual tank waste for chemical and radionuclide content. Additional treatments may be required if the measured inventory does not meet regulatory requirements. After removal of the contents to acceptable levels, closure activities fill the tanks with a grout to isolate the residual solids and limit transport into the environment.

Presently, characterization of tank residuals requires collection of discrete samples from a tank with subsequent characterization at an onsite analytical laboratory. The entire sampling and analytical measurement process is time consuming, labor-intensive, and exposes site workers to radiation doses. The tank environment often requires the design and fabrication of a one-of-kind sampling tool for each tank, which is discarded after each use. In-situ characterization of tank residuals is an attractive alternative. For successful deployment of a spectroscopic system, the equipment must be able to function for an acceptable period under high radiation fields, high humidity, and in strongly corrosive environments.

An early attempt to deploy a Raman optical system into a waste tank included using a cone penetrometer drilling technology.[4] The cone penetrometer was originally developed for geological and groundwater applications but it was adapted to host fiber and glass optics to deliver and receive light. The combined Raman-Cone Penetrometer technology detected organics in a few grams of archived sludge but discrepancies in selecting a representative sample and accuracy problems prevented the deployment of this technology in scaled-up real waste tanks. In 2012, SRNL and EIC Laboratories evaluated a prototype Raman telescope constructed by EIC, with a capability for remote measurements up to 50 feet away from the device, for its suitability in making in situ Raman measurements of tank contents. The telescope combines optics for delivery and focusing of the Raman excitation laser and collection of the Raman scattering signal with a video camera for imaging of the sample and improved focusing of the Raman laser. Topics covered in the evaluation included general performance at a range of standoff distances from the solids sampled, ability to measure simulated solid waste samples, and the sensitivity to radiological (gamma) exposure.

Figure 1 depicts the Raman telescope system. The design contains a laser (HeNe, 632 nm, ~100 mW continuous wave) spectrometer, and cooled CCD array detector in a unit remote from the sampling area. An optical fiber couples the laser light and brings it to the telescope. The telescope consists of a cylindrical housing that hosts a movable microscope objective and a fixed lens, which in combination allow for adjustment of the far field focal distance. The focused laser spot size was ~5 mm. This Galilean design is better suited than Newtonian or Cassegrain-Schmidt designs[5] for deployment in SRS tank risers due to its smaller diameter and relative mechanical simplicity. The telescope also has an exterior window for protection of the interior components.

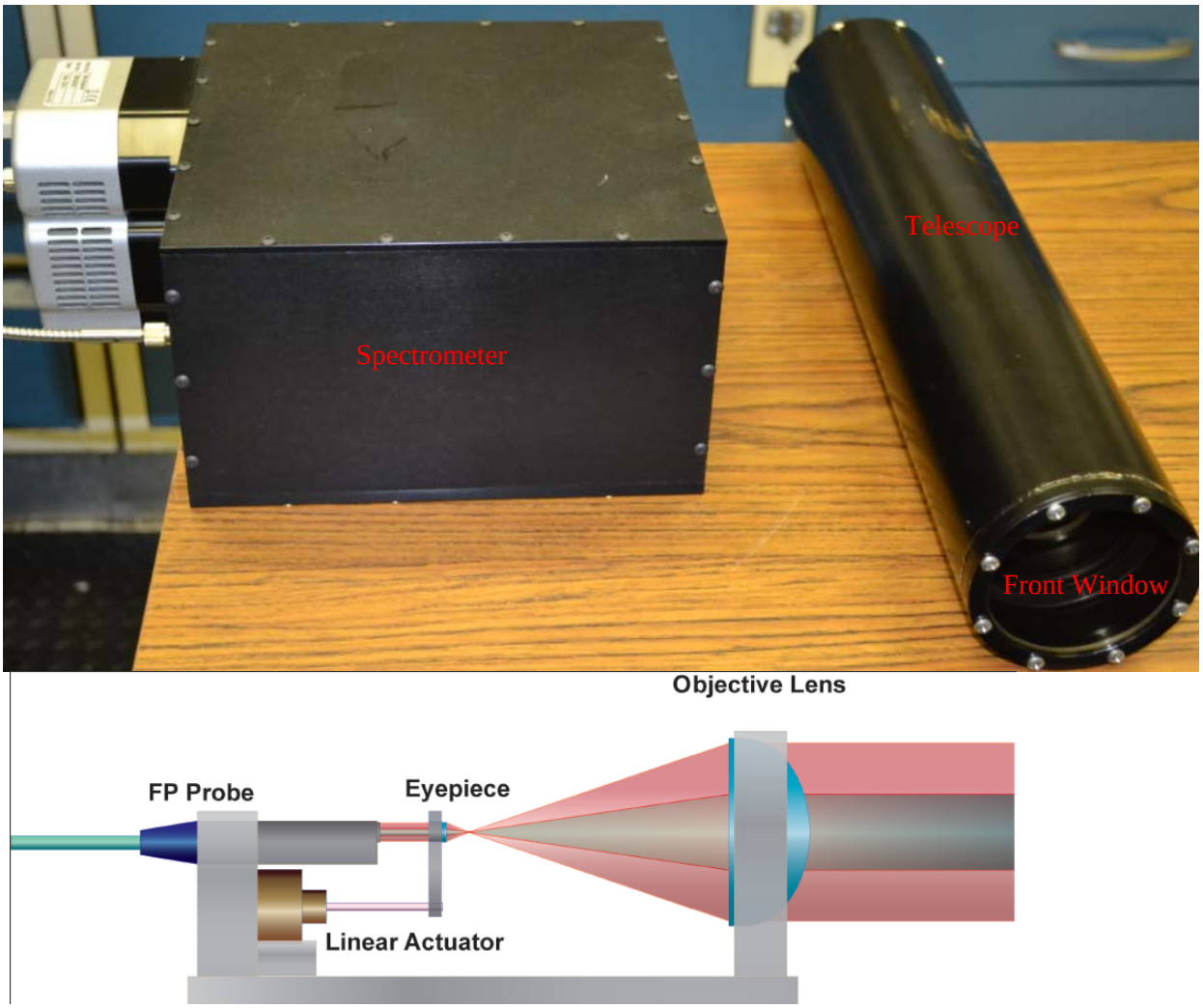

Figure 1. Photograph of the Raman telescope and spectrometer

A linear actuator controls the positioning of the eyepiece in the telescope remotely, with the condition of laser focus confirmed by observation of the laser spot on the sample using a video camera system. The camera operates in parallel to the laser system and transmits through the front window.

Initial testing observed Raman spectra of powdered sodium nitrate and ground simulated salt cake at distances ranging from 10 – 50 feet. Testing contained the solid samples in square-sided glass bottles. Figure 2 compares spectra of sodium nitrate at 10 and 50 feet. The material is clearly identifiable, with an expected decrease in signal associated with a smaller solid angle of scattering at the longer distance.

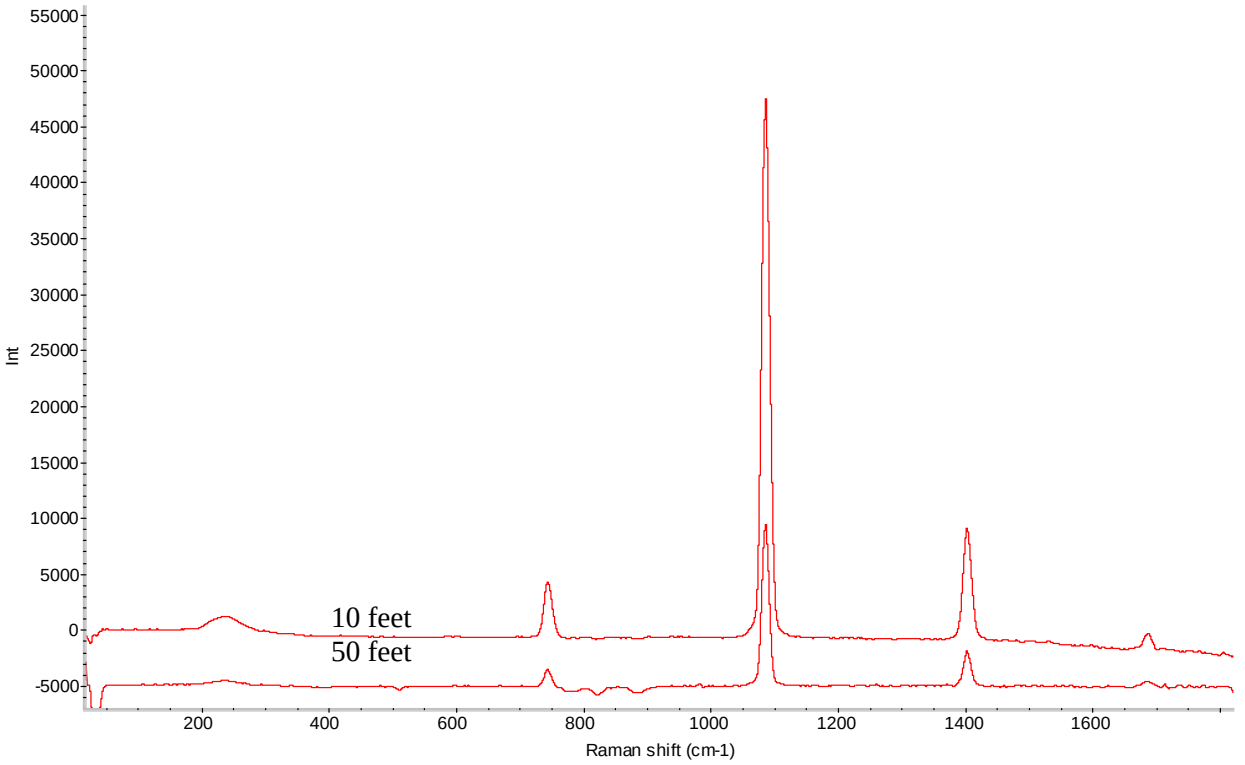

Figure 2. Raman spectra of powdered $NaNO_3$ obtained with the Raman telescope at 10 and 50 feet.

As Figure 3 shows, the decrease of signal with increased distance is more pronounced for the salt cake sample. However, other differences in the spectra suggest that additional factors may influence these two spectra. The primary nitrate peak has shifted between the two spectra, and there is fluorescence in the shorter distance spectrum that is not evident in the longer distance spectrum. The most likely explanation for this observation is that, despite best efforts at alignment, the laser was sampling a different spot in an inhomogeneous sample. Also, the laser depth of focus at these distances is on the order of a few mm, which makes accurate focusing difficult, especially for the longer focusing distances. Testing showed that slight variances in focal distance, either into the bulk or in front of the surface of the solid sample, caused a drastic decrease in Raman signal. Both factors were exacerbated by relocation of the telescope between the 10 and 50 foot measurements, making alignment differences more likely. Extremely fine adjustment of the eyepiece position is required to optimize the focal position. Likewise, accuracy of the video imaging system is critical to achieve laser focus in a real application.

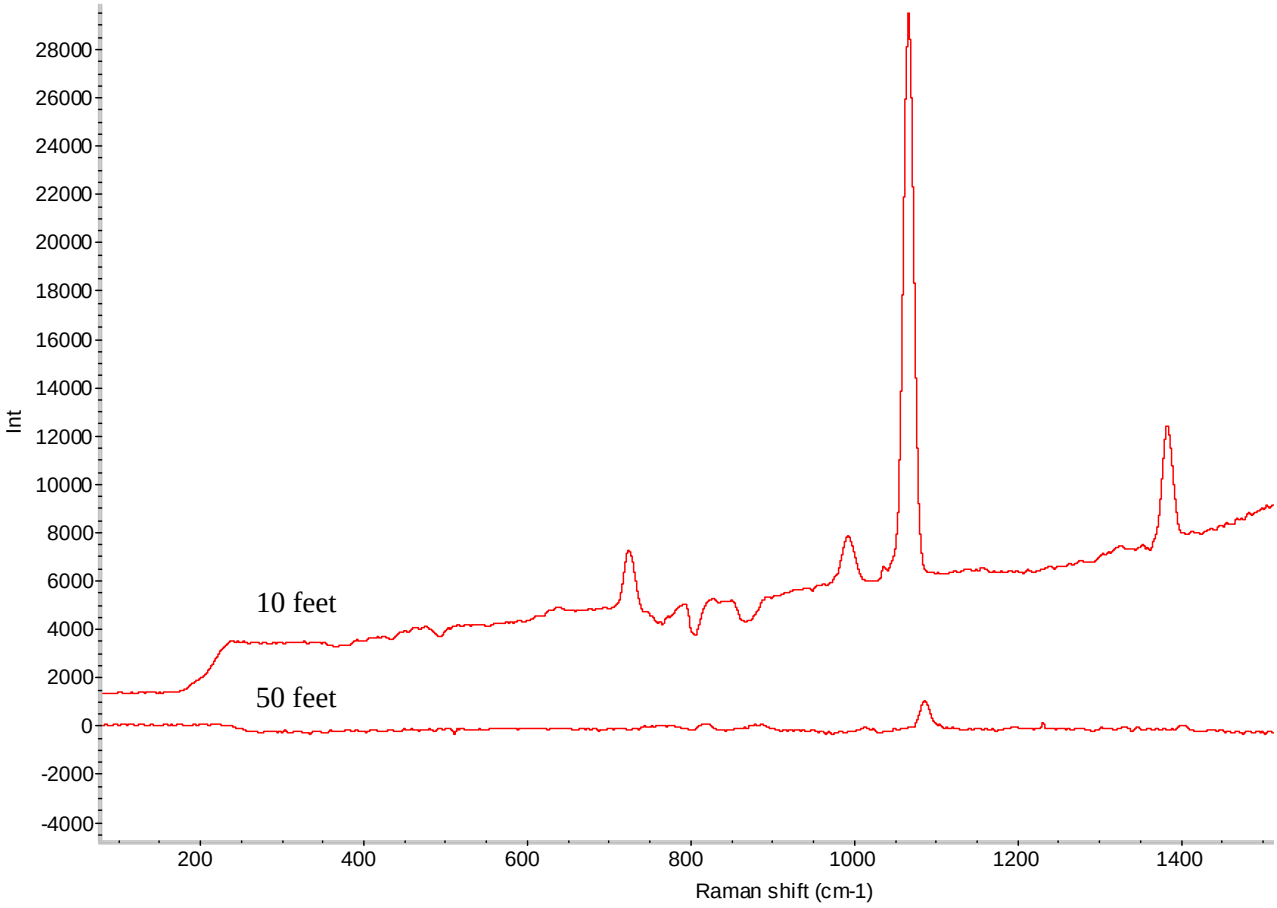

Figure 3. Raman spectra of powdered saltcake simulant obtained with the Raman telescope at 10 and 50 feet.

In addition, the project examined radiation resistance of the telescope by exposing the assembly to a Co-60 gamma source at SRNL for increasing time. After each irradiation, personnel reconnected the telescope to the spectrometer unit and measured sodium nitrate powder at a standoff distance of 10 feet. The testing also assessed mechanical and video functioning after each dose. The comparatively large size of the telescope and its placement in the irradiation chamber resulted in different parts of the assembly receiving different doses, with the highest doses absorbed by the front window (~1.06 x 10^4 rad/h) and the lowest at the back end of the telescope (~2.27 x 10^3 rad/h). The cumulative exposure time was 34.5 hours for a maximum total dose of 3.7 E5 rad at the front window of the telescope.

Figures 4 (spectra) and 5 (peak area) show an example of the effect of cumulative dose on the Raman spectrum of sodium nitrate. Similar trends occurred for other sodium nitrate peaks (not shown). In all cases, the intensities of the bands decreased substantially, with all other factors (e.g., laser power, integration time, etc.) held constant. Figure 6 shows the discoloration of the front (non-focusing) window of the telescope after the complete dose. The discoloration of this window (a borosilicate glass) is the largest single factor in the decrease of the Raman signal. Transmission of the laser through the darkened window decreased by 17% compared to removal of the window. The next generation telescope uses a radiation-hardened quartz window for longer service.

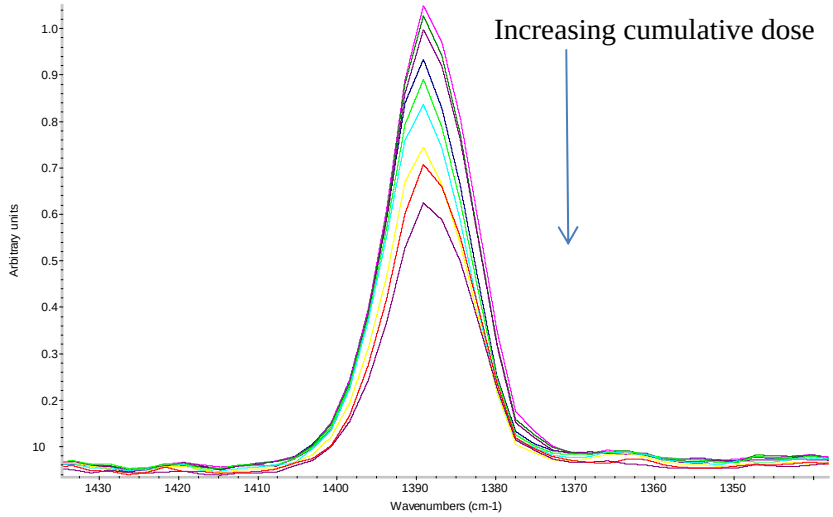

Figure 4. The effect of radiological dose on the 1388 cm^{-1} sodium nitrate peak.

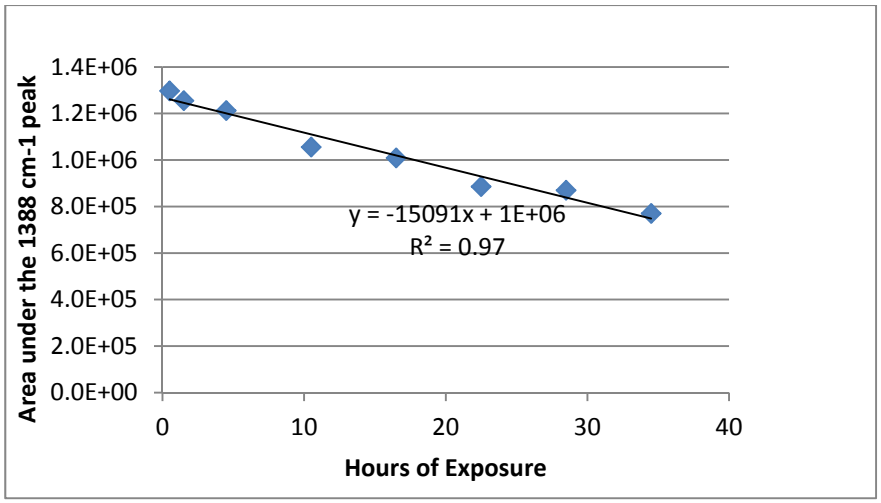

Figure 5. Dependence of peak area on exposure time for the 1388 cm^{-1} sodium nitrate peak.

Figure 6. Photograph of the front window showing the darker, amber color after 34.5 hours of exposure.

Overall loss of the Raman signal reached ~40% after the full dose. In addition to the effects of window darkening, further loss of signal resulted from the inability to refocus the telescope to the sample at 10 feet. The linear actuator froze, with the focus fixed at 19.1 feet. Note that testing could still obtain the video signal at this cumulative dose; however, the decreased transmission of the window required external illumination of the sample with a LED flashlight to get a full image.

The observed loss of performance with radiative dose could be mitigated through a better choice of materials. Substitution of regular borosilicate glass with quartz, and the use of non-organic lubricants, will remove those materials that are most susceptible to the effects of gamma irradiation. Conversely, the radiation levels inside a tank are much higher than those explored in this scoping study, and it is reasonable to assume that even with better materials, the telescope will eventually become unusable. Thus, planning for an application must consider the expected lifetime of the system to define projected maintenance periods and protocols.

The variable signal obtained with the telescope of the salt cake sample also suggests that sampling issues require additional development and testing before a deployment in nuclear service. The issues include both the ability to get a reproducible signal, due to the tight tolerances for optimal focus, and the inhomogeneous nature of the sample itself. Testing obtained strong signals for the pure, clean sodium nitrate sample, but variations in color, surface quality and distribution could lead to problems in seeing minor (or even semi-major) components in actual tank waste.

2.2 Raman Liquid Probe Testing

In 2007, SRNL explored the feasibility of using a fiber-based Raman probe for in situ monitoring of oxyanions in various processes at SRS. One potential application involved real-time monitoring of the filtrate during tests of a rotary microfilter. Tracking of decreasing nitrate concentrations served as a measure of the completeness of the washing process and potentially as a way to detect filter breakthrough. The tracking would allow for the use of a minimal volume to reach the washing endpoint, and could support an increased rate of throughput. Another potential application involved detection of multiple chemical endpoints in leaching and evaporation operations. This scoping work was conducted in conjunction with flowsheet development work on sludge batch simulants. This application proved more challenging due to large amounts of entrained solids that interfered with the Raman signal obtained from the solution phase.

Developed by Brian Marquardt, CPAC / U. Washington

Figure 7. Ball lens Raman probe used in liquid analysis test.

The most notable aspect of the fiber probe used in these tests is that it terminated in a ball lens (see Figure 7). The sampling volume for this arrangement is localized to a very small region at the tip of the lens. This design assumed that this configuration would provide the most consistent sampling volume for dissolved analytes in the presence of bubbles and solids. The spectrometer used for these tests was a low-grade instrument with lesser sensitivity and higher noise characteristics than the instrument described in the previous section. Therefore, the detection limits and reliability observed in these tests are not an absolute limitation for these methods with currently available technology. The performance characteristics of the measurement system can be tailored to the application.

The results from testing of the probe for nitrate detection in a flowing stream with few or no particulates are promising. Figure 8 shows the calibration curve for nitrate. For a 1 minute acquisition time with 180

mW excitation at 785 nm, the system had a detection limit of less than 800 ppm and a measurement error of ~1.2% for concentrations greater than 2400 ppm. Sample results in flow also agreed well (~5%) with grab sample analyses for cases when entrained air bubbles did not affect the analysis (see Figure 9). Testing showed an effect of bubbles for any probe insertion point with flow perpendicular to the probe. The effect of the bubbles could be cleared with continual tapping of the probe to dislodge any bubbles nucleating on the probe end. Personnel subsequently learned that other researchers had found that insertion of the probe to point directly into the flow direction provides less opportunity for bubble persistence. Alternately, a degassing arrangement in the flow stream could remove the problem.

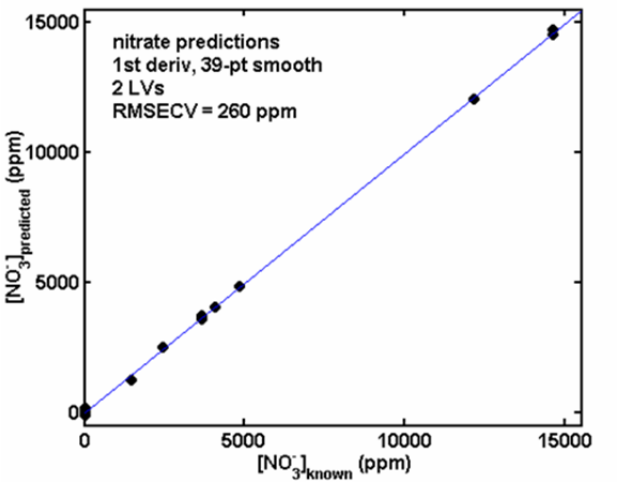

Figure 8. Calibration curve for nitrate, obtained using the ball lens probe.

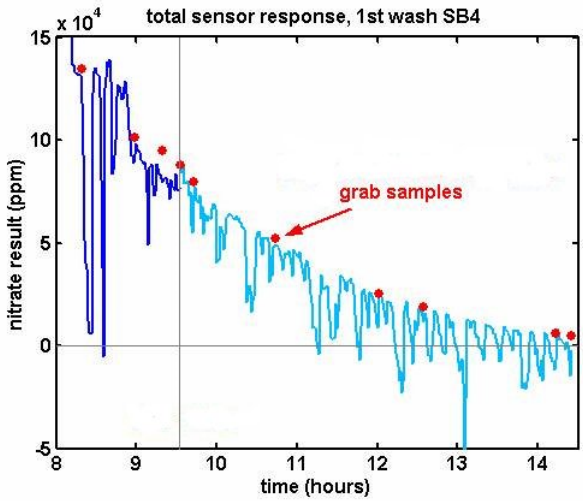

Figure 9. Nitrate readings for filtrate wash run, showing the effect of bubbles on the signal.

The efforts to measure nitrate and other anions in the supernate of slurries proved less successful, due to the high solids load (20-30%). At these levels, almost all of the sampling volume was occupied by the solids, and even high anion concentrations (>40,000 ppm) could barely be seen in the spectra. The authors considered a self-cleaning “push-pull” filtration system as a possible alternate to allow the probe to access relatively clean solution, but the scope of the project did not permit development of this device. Other factors recognized as requiring future work include: a correction for sample absorbance, which would

attenuate both the laser and Raman scattering intensities; corrections for variations in solution ionic strength and temperature, which lead to shifts in the Raman line positions and line shapes; and recognition of potential spectral overlaps for several anions expected in these solutions (e.g., nitrate and carbonate, nitrite and formate), which can introduce significant calibration errors if not considered. Calibration design can accommodate all of these factors with sufficient care.

Another performance area that needs further consideration is the laser power endurance of the Raman system. The Raman system may be deployed continuously for several months and during that time the laser power will decline. The current strategy that is used to account for laser power loss is to normalize all recorded Raman peaks to the OH-stretch Raman peak from water. Since the hydrogen bonding state of water varies with its salt ionic strength, the OH-stretch Raman peak of water may vary with solution composition and it adds variance to the Raman quantitative measurement.

2.3 Raman Gas Analysis Testing

2.3.1 Aluminum Cladding Dissolution Testing

SRNL is currently using Raman spectroscopy to monitor gaseous emissions associated with metal dissolution in nitric acid. These experiments are specifically relevant to processing of irradiated nuclear materials in SRS's H Canyon and HB-Line facilities, but the capabilities demonstrated here are applicable to other nuclear waste processing scenarios where real time, in situ detection of flammable or corrosive gases can help avoid process upsets. The equipment used here incorporates fiber coupling of the laser and spectrometer to a gas cell mounted downstream of the dissolution vessel, through which purge and evolved gases continually flow. The spectrometer utilizes an array detector and is able to follow the concentrations of several gases simultaneously (e.g., H_2, N_2O, NO, H_2O, CO, CO_2, and NO_2).

One example follows. In this application, an aluminum coupon, with a mercury catalyst, is dissolved in 9 M nitric acid in a purged vessel. The system is calibrated to follow concentrations of H_2, O_2, N_2, NO, NO_2, and N_2O. Figure 10 shows the trend of these species throughput the dissolution, represented as a proportion of the total amount of evolved gas. The labels indicate various events. At approximately 12 minutes, the purge gas changes from Ar to N_2. Soon thereafter, as the temperature reaches the boiling point, substantial amounts of NO evolve, with smaller amounts of H_2 and N_2O. Figure 11 shows the Raman spectrum at 21 minutes, with clear peaks for each of the four Raman-active species (N_2, NO, N_2O, and H_2). When the Hg catalyst is injected at approximately 27 minutes, the gas evolution rate increased dramatically, as evidenced by the drop in N_2 composition. At this point, the N_2O/NO ratio increases, and H_2 and NO_2 levels also increase. The dissolution rate begins to decrease at about 32 minutes, and ends at about 45 minutes when the heating unit is turned off. At 49 minutes, the vessel is opened to air, and then returned to an Ar purge at 57 minutes. Variations in the Raman laser power is accounted for by normalizing the Raman N_2 stretch peak of air for every spectrum collected.

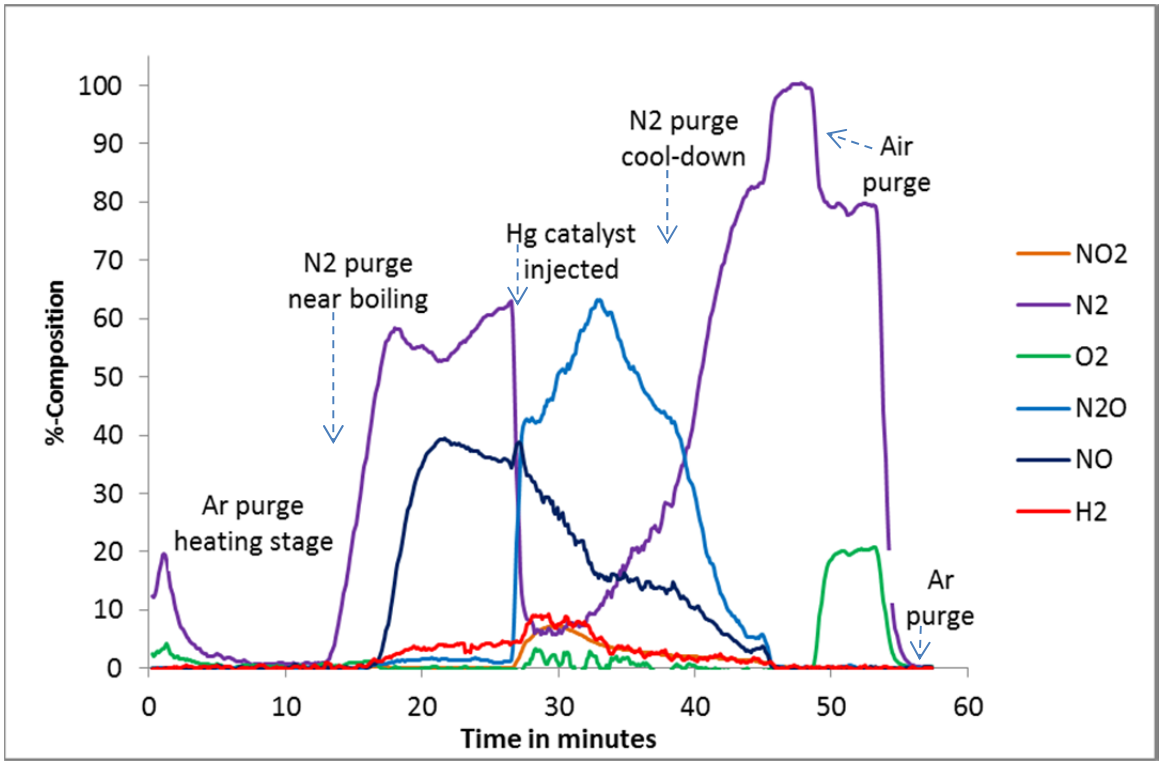

Figure 10. Evolution of gas species during aluminum coupon dissolution, as followed by Raman spectroscopy.

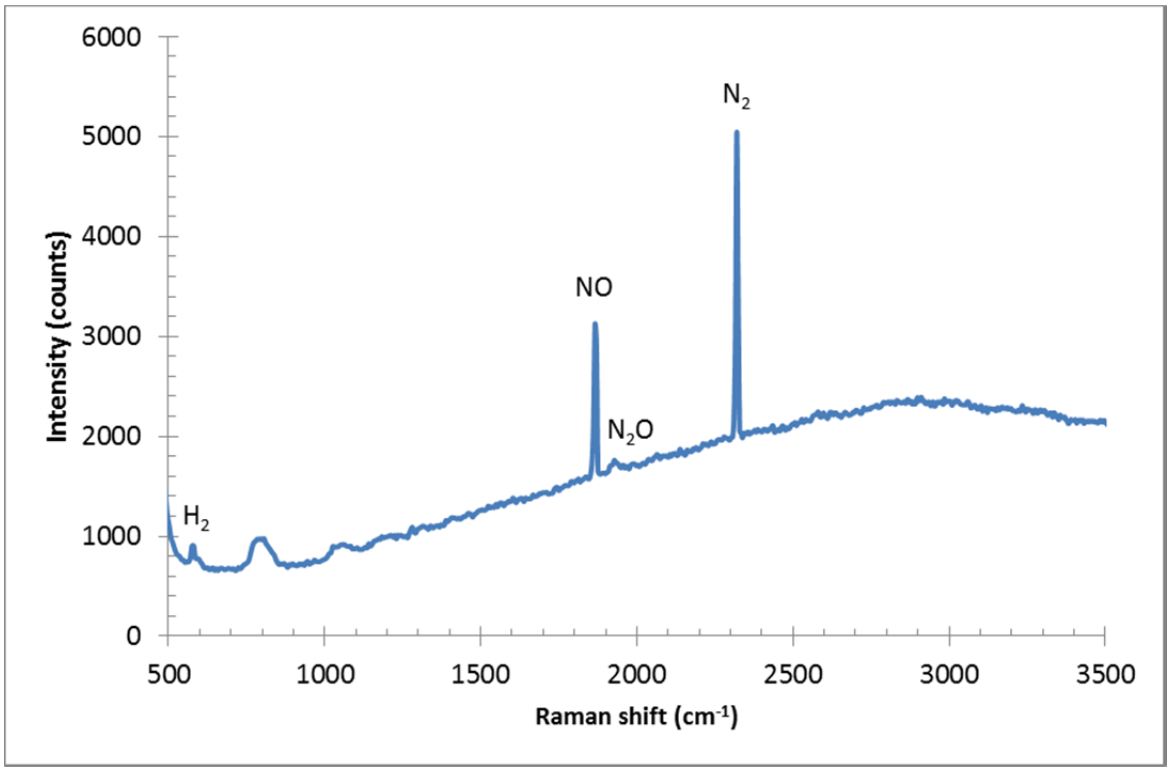

Figure 11. Raman spectrum of evolved gases at 21 minutes.

2.3.2 Solvent Extraction Vapor Concentration

In another set of experiments, SRNL tested a multi-pass gas cell to monitor the gas phase above a Caustic-Side Solvent Extraction (CSSX) solvent heated at different temperatures. The multi-pass configuration reflected the 632 nm laser signal at least four times in the area of gas analyzed (see Fig. 12).

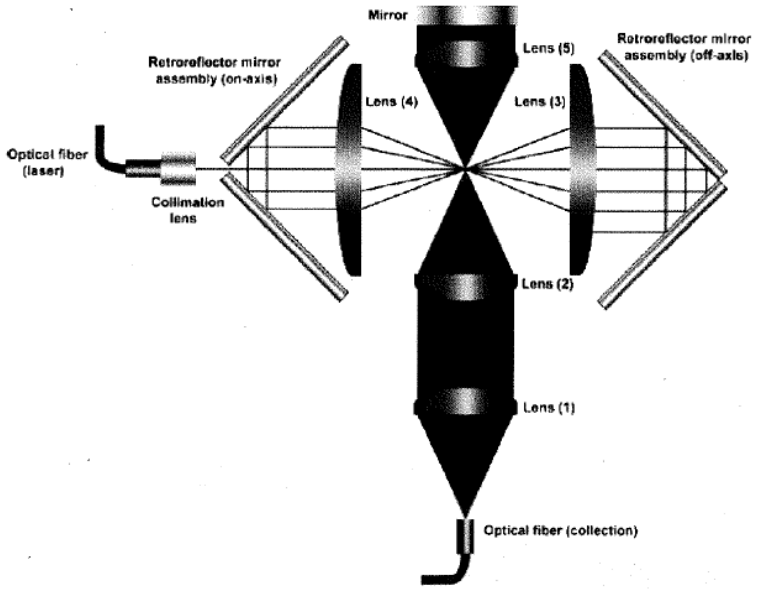

Figure 12. A schematic of the multipass Raman gas cell

Personnel placed approximately 15 mL of CSSX solvent in a sealed glass vessel with the overhead pipe connected to the multi-pass Raman gas cell and heated to different temperatures (i.e., 27, 44.5, 47.2, 51.3, and 53.6 °C). Testing purged the vapor space with air to deliver the gas to the multi-pass gas cell. A 300 mW laser was delivered to the multi-pass cell and the scattered Raman light was collected for 60 seconds. Figure 13 displays the observed data.

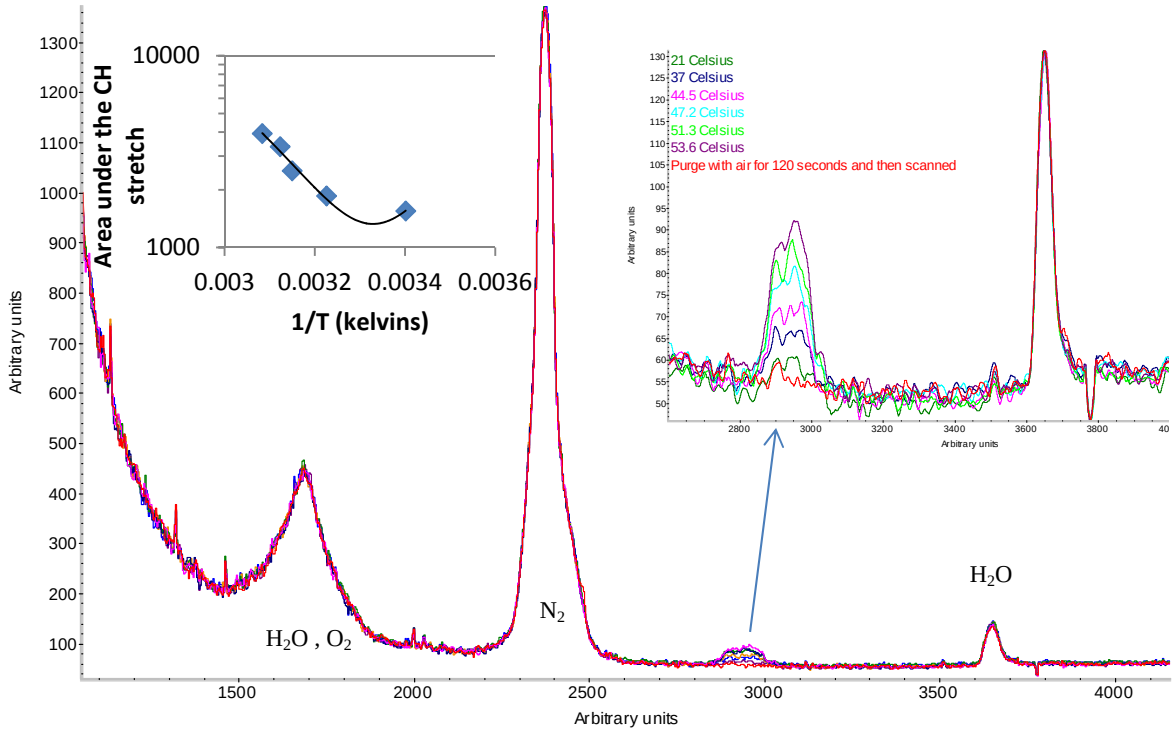

Figure 13. A set of Raman spectrum of the overhead of a heated CSSX solvent using the multipass Raman gas cell and integrating for 60 seconds.

Figure 13 shows the Raman scattering peaks of the purge gas and of the volatile component of CSSX, Isopar™L. Further arithmetic manipulation of the spectrum shows the CH stretch peak associated with the Isopar™L obeys Arrhenius theory (or Antoine's theory) of vapor pressure with temperature. Overall, the multi-pass gas Raman cell can be deployed to monitor the gas phase of processes that may generate gases with significant risk to safety or to the health of the environment.

3.0 Conclusions

SRNL has conducted several studies using Raman spectroscopy to analyze materials of potential interest for in situ monitoring of radiological waste processing. Testing examined solids, liquids, and gases in a variety of process applications. Raman telescopes for analysis inside storage tanks require substantial development to reach maturity for a deployment in radiological service. The ability to operate the telescope remotely, the ruggedness of the components to the high radiation fields in the tanks, and the amenability of the materials to Raman analysis all pose significant challenges. In situ analysis of liquids and gases is more feasible, especially if sampling avoids mixed-phase samples (e.g., gas or solids entrained in a liquid, or condensation in a gas). Based on SRNL experience, some development is required for a liquid analysis; however, we note that in the near-decade since the reported work occurred, both SRNL and the scientific community have improved capabilities substantially. The gas analysis work described here is ready for application to other problems with a minor amount of development (e.g., engineering interfaces, software integration with a facility, and process-specific calibrations).

4.0 References

[1] L. W. Gray, M. Y. Donnan, and B. Y. Okamoto, "Chemical Characterization of SRP Waste Tank Sludges and Supernates", DP-1483, August 1979.
[2] C. T. Johsnston, S. F. Agnew, J. R. Schoonover, J. W. Kenney, III, B. Page, J. Osborn, and R. Corbin, "Raman Study of Aluminum Speciation in Simulated Alkaline Nuclear Waste", Environ. Sci. Technol., (2002), 36, 2451-2458.
[3] M. Lenoir, A. Grandjean, S. Poissonnet,, and D. R. Neuville, "Quantitation of sulfate solubility in borosilicate glasses using Raman Spectroscopy", J. of Non-Crystalline Solids 335 (2009), 1468-1473.
[4] K. R. Kyle, S. Weeks, J. Bello and S. B. Brown, "Raman Probe", OST Reference #1544, DOE/EM-0442, July 1999.
[5] D. W. Ball, "The Baseline Telescope Optics", Spectroscopy (2005), 20(1), 52-54

Distribution:

D. E. Dooley, 999-W
T. B. Brown, 773-A
D. H. McGuire, 999-W
S. D. Fink, 773-A
C. C. Herman, 773-A
E. N. Hoffman, 999-W
F. M. Pennebaker, 773-42A
A. L. Washington, II, 773-42A
W. R. Wilmarth, 773-A
Records Administration (EDWS)

P. R. Jackson, DOE-SR, 703-46A

F. F. Fondeur, 773-A
D. T. Hobbs, 773-A
R. J. Lascola, 999-2W
P. E. O'Rourke, 773-A
M. J. Barnes, 773-A
C. M. Gregory, 773-A
E. T. Sadowski, 773-A

M. Wentink, BNI, Hanford WTP